AMERICAN SOCIETY FOR MICROBIOLOGY | Journal of Virology

Virology | Full-Length Text

Biologically significant interaction of human herpesvirus 8 viral interferon regulatory factor 4 with ubiquitin-specific protease 7

Zunlin Yang,[1] **John Nicholas**[1]

AUTHOR AFFILIATION See affiliation list on p. 17.

ABSTRACT Human herpesvirus 8 (HHV-8), associated with Kaposi sarcoma, primary effusion lymphoma (PEL), and multicentric Castleman disease, encodes four interferon regulatory factor homologs, vIRFs 1–4, that interact with and inhibit various mediators of host-cell defense against virus infection. A cellular protein targeted by all the vIRFs is ubiquitin-specific protease 7 (USP7); while replication-modulatory and latently infected PEL-cell pro-viability phenotypes of USP7 targeting have been identified for vIRFs 1–3, the significance of the interaction of vIRF-4 with USP7 has remained undetermined. Here we show, through genetic ablation of the vIRF-4-USP7 interaction in infected cells, that vIRF-4 association with USP7 is necessary for optimal expression of vIRF-4 and normal HHV-8 replication. Findings from experiments on transfected and infected cells identified ubiquitination of vIRF-4 via K48-linkage and USP7-binding-associated suppression of vIRF-4 ubiquitination and, in infected cells, increased vIRF-4 expression. Analysis of IFN-I induction and associated signaling as a function of vIRF-4 and its interaction with USP7 identified a role of each in innate-immune suppression. Finally, activation via K63-polyubiquitination of the innate-immune signaling mediator TRAF3 was found to be suppressed by vIRF-4 in a USP7-binding-associated manner in infected cells, but not in transfected cells, likely via binding-regulated expression of vIRF-4. Together, our data identify the first examples of vIRF ubiquitination and a vIRF substrate of USP7, enhanced expression of vIRF-4 via its interaction with USP7, and TRAF3-inhibitory activity of vIRF-4. The findings address, for the first time, the biological significance of the interaction of vIRF-4 with USP7 and reveal a mechanism of vIRF-4-mediated innate-immune evasion and pro-replication activity via TRAF3 regulation.

IMPORTANCE HHV-8 homologs of cellular interferon regulatory factors (IRFs), involved in host-cell defense against virus infection, interact in an inhibitory fashion with IRFs and other mediators of antiviral innate immunity. These interactions are of demonstrated or hypothesized importance for successful primary, productive (lytic), and latent (persistent) infection by HHV-8. While HHV-8 vIRF-4 is known to interact physically with USP7 deubiquitinase, a key regulator of various cellular proteins, the functional and biological significance of the interaction has not been addressed. The present study identifies the interaction as important for HHV-8 productive replication and, indeed, for vIRF-4 expression and reveals a new function of vIRF-4 via inhibition of the activity of TRAF3, a pivotal mediator of host-cell antiviral activity through activation of cellular IRFs and induction of type-I interferons. These findings identify potential targets for the development of novel anti-HHV-8 agents, such as those able to disrupt vIRF-4–USP7 interaction or vIRF-4-stabilizing USP7 activity.

KEYWORDS viral interferon regulatory factor, vIRF-4, human herpesvirus 8, ubiquitin-specific protease 7, ubiquitination, TRAF3, lytic replication

Editor Jae U. Jung, Lerner Research Institute, Cleveland Clinic, Cleveland, Ohio, USA

Address correspondence to John Nicholas, nichojo@jhmi.edu.

The authors declare no conflict of interest.

See the funding table on p. 17.

Received 5 February 2024
Accepted 19 April 2024
Published 16 May 2024

Kaposi sarcoma (KS)-, primary effusion lymphoma (PEL)-, and multicentric Castleman disease-associated human herpesvirus 8 (HHV-8, formally human gammaherpesvirus 8) was the first virus identified to encode homologs of interferon regulatory factors (IRFs). The four viral IRFs (vIRFs) are expressed during productive (lytic) replication, but in the context of PEL cells, vIRFs 1, 2, and 3 are also expressed during latency (1–3). Latency-associated expression of vIRF-1 mRNA has been reported in at least some cases of KS, indicating that it may be expressed independently of lytic replication in infected KS endothelial cells (4). HHV-8 vIRFs have been reported to interact in an inhibitory fashion with a variety of cellular proteins involved in innate immunity, stress signaling, and apoptosis. Protein targets include cellular IRFs (bound by vIRFs 1–4), IRF-interacting transcriptional co-activators pCBP/p300 (vIRFs 1–3), antiviral signaling proteins STING and MAVS (vIRF-1), pro-apoptotic p53 (vIRFs 1 and 3) and BH3-only proteins Bim and Bid (vIRF-1), and p53-suppressing MDM2 E3 ubiquitin ligase (vIRF-4) (5–8). On the basis of such findings, it is believed that vIRFs function, at least in part, to inactivate innate cellular defenses against infection, latency establishment, and/or virus replication. However, very few of the many reported interactions have been detected and assessed functionally in the context of infected cells. Of note is that the eight vIRFs of rhesus rhadinovirus (closely related to HHV-8) have been shown collectively, via genetic and *in vivo* analyses, to be required for normal primary infection and latency establishment and to act via suppression of antiviral innate and adaptive immune responses (9). It is likely that HHV-8 vIRFs act similarly, in addition to having specific individual functions beyond immune evasion (5, 6).

Specific to vIRF-4 are its physical and functional interactions with Notch transcription factor co-activator CSL, cell-cycle gene-targeting transcription factor β-catenin, and the HHV-8 immediate–early transcriptional activator RTA (10–12). The latter two interactions are thought to promote virus productive replication by suppression of cell cycle progression via inhibition of cyclin D1 (and related) gene expression (11) or through enhanced expression of RTA-induced viral lytic genes, including vIRF-1 and vIRF-4 (12). The latter study demonstrated, via vIRF-4 depletion in infected iSLK epithelial cells, the importance of vIRF-4 for HHV-8 productive replication. Another target of vIRF-4, in common with all other HHV-8 vIRFs, is ubiquitin-specific protease 7 (USP7) (13–16). USP7 is best known for its targeting, deubiquitination, and consequent stabilization of p53 and its E3 ubiquitin ligase, MDM2, with the balance between these determining the levels of p53 and associated stress signaling (17). Activation and stabilization of p53 occur in response to virus infection and replication, and these cellular processes need to be regulated by the action of viral proteins to enable successful virus infection and production (18–20). Through genetic analyses in virus-infected cells, vIRF-1 targeting of USP7 was found to promote HHV-8 productive replication, whereas interactions of vIRF-2 and vIRF-3 with USP7 were revealed (counterintuitively) to inhibit replication (14, 15, 21). An elegant structural study reported vIRF-4 interaction with USP7 via two interfaces, canonical through vIRF-1 ASTS and N-terminal (TRAF-domain) USP7 sequences and also by contacts between ASTS-neighboring vIRF-4 residues and the USP7 catalytic domain (16). The same report demonstrated the suppression of USP7 activity and induction of p53 and apoptosis in HHV-8$^+$ PEL cells by peptides incorporating the USP7-binding residues of vIRF-4 (16). However, the functional consequences of vIRF-4–USP7 interaction and its role in virus biology are unknown.

Here, we report the significance of USP7 targeting by vIRF-4 for HHV-8 productive replication and demonstrate that this is mediated, at least in part, through USP7-enhanced expression of vIRF-4 and vIRF-4-mediated suppression of cellular innate-immune signaling. We provide the first evidence of a vIRF substrate of USP7 and of biologically significant regulation of vIRF-4 via its interaction with the deubiquitinase.

RESULTS

Phenotypic analyses of the interaction of vIRF-4 with USP7

While it has been reported that vIRF-4 interacts directly with USP7 and that peptides incorporating USP7-interacting residues of vIRF-4 suppress PEL cell growth (16), the significance of vIRF–4-USP7 interaction in HHV-8 biology is unknown. To address this issue, we sought first to derive vIRF-4 variants defective for the interaction with USP7 and then incorporate corresponding mutations into the HHV-8 genome for phenotypic analyses. Previous crystallographic data identified two adjacent sites of vIRF-4 contact with USP7: one comprises a canonical USP7-binding motif, $ASTS_{214}$ (matching the A/PxxS consensus sequence), and the second contains the core sequence TWR_{233} (16). STS_{214} and TWR_{233} were changed to alanine residues via appropriate translation-codon mutations (Fig. 1A). Expression vectors were generated to express Flag-tagged versions of these proteins along with chitin-binding domain (CBD)-fused USP7 in cotransfected cells. Lysates of transfected cells were used for Flag-immunoprecipitation (IP) or CBD-based affinity-precipitation (AP) of the respective proteins. Reciprocal coprecipitations of USP7 and vIRF-4 identified the interaction of vIRF-4 with USP7 and greatly diminished or abrogated interaction resulting from the introduced $STS_{214}AAA$ (STS^X) and $TWR_{233}AAA$ (TWR^X) mutations (Fig. 1B).

We next generated HHV-8 recombinant genomes encoding each vIRF-4 variant in the context of the BAC16 HHV-8 bacmid (22) by using established recombineering techniques (23). Wild-type-reverted genomes were generated as controls for phenotypic experiments. We also generated BAC16 genomes encoding Flag-tagged versions of wild-type and the USP7-binding motif-mutated vIRF-4 proteins to use in subsequent analyses (see below). Each of the genomes was assessed for overall integrity by restriction analysis (Fig. 1C). The respective genomes were transfected into iSLK cells (24), inducible with doxycycline (Dox) for expression of the viral RTA lytic activator, and the corresponding viruses were recovered via Dox and sodium butyrate (NaB) treatment of the cultures and titered using standard techniques (see Materials and Methods).

Normalized infectious doses of the parental (WT) and binding-motif-mutated (STS^X; TWR^X) and repaired control (STS^R; TWR^R) viruses were used to infect parallel iSLK cultures, latently infected ($BAC16^+/Hyg^r$) cells selected by hygromycin treatment, and cell lysates analyzed by immunoblotting for HHV-8 LANA to verify equivalent viral loads (Fig. 1D). The cultures were then treated with Dox and NaB to induce lytic replication, and media were harvested for determinations of cumulative virus yields over the course of 6 days. Cell-released, encapsidated (DNase I-resistant) viral genome titers were determined by qPCR. The data revealed significant suppression of virus replication by each of the introduced mutations, with a greater effect of TWR^X, and restoration of replicative competence in the repaired viruses (Fig. 1E).

USP7 targeting by vIRF-4 in the regulation of antiviral signaling

We have reported previously that vIRF-2 regulates TRAF3- and TRAF6-mediated signal transduction by interacting competitively with the TRAFs for USP7 binding, leading (biologically unintuitively) to increased TRAF3 and TRAF6 activity and promoting interferon type I (IFN-I) induction and resulting antiviral effects (15). In view of the previous findings, we used a luciferase-based reporter assay to test for the potential effect of vIRF-4 on interferon-sensitive response element (ISRE)-driven transcription. In the context of HHV-8-infected iSLK cells transfected with the ISRE-luciferase reporter, we found that luciferase expression was significantly increased by both the STS^X and TWR^X mutations and restored by repair of the mutations (STS^R; TWR^R) (Fig. 2A). Notably, however, the mutations did not relieve vIRF-4 suppression of reporter activity stimulated by IFN-inducing MAVS (Fig. 2B) or directly by IFN-β treatment (Fig. S1A) in the context of transfected 293T cells, and native and variant vIRF-4 proteins were active in USP7-null 293T cells (Fig. S1B). These data indicate that the observed effects of the mutations in infected cells may be due to factors affecting vIRF-4 expression, negated in

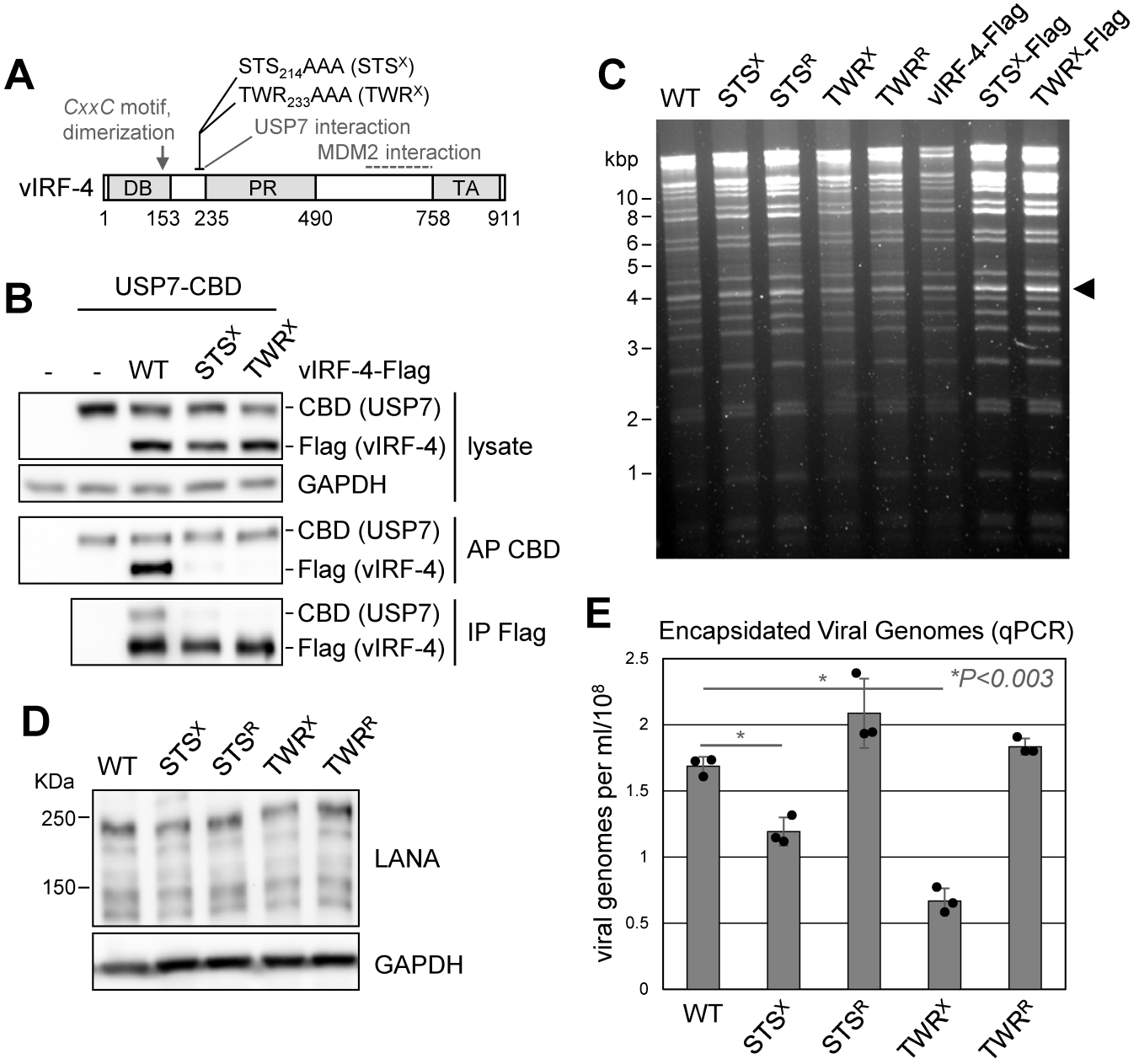

FIG 1 Contribution of vIRF-4-USP7 interaction to HHV-8 productive replication. (A) Diagrammatic representation of vIRF-4, showing DNA-binding (DB), proline-rich (PR), and transactivation (TA) domains; regions of protein interaction; and introduced mutations. (B) Assessment via transfection-based coprecipitation assays of the effects of vIRF-4 mutations $STS_{214}AAA$ (STS^X) and $TWR_{233}AAA$ (TWR^X) on the interaction of vIRF-4 with USP7. Flag-tagged vIRF-4 and chitin-binding domain (CBD)-fused USP7 were coexpressed from plasmid vectors in transfected 293T cells, and the proteins were isolated from cell lysates by immunoprecipitation (IP) or affinity-precipitation (AP), and coprecipitates were analyzed by immunoblotting. (C) Restriction (HindIII) analysis of wild-type (WT), vIRF-4 ORF-mutated (STS^X; TWR^X), and WT-reverted (STS^R; TWR^R) BAC16 HHV-8 genomes, along with those engineered to express Flag-tagged WT, STS^X, and TWR^X vIRF-4. The arrowhead indicates the position of the band containing the vIRF-4 coding sequences. (D) Verification by immunoblotting of equivalent levels of latency-associated nuclear antigen (LANA) expression, indicative of latent viral load, in iSLK cultures infected with equal infectious doses of vIRF-4 ORF-mutated (STS^X; TWR^X) and repaired (STS^R; TWR^R) viruses. GAPDH was used as a loading and normalization control. (E) Viruses produced over 6 days from Dox/NaB-treated (lytically reactivated) cultures harboring the respective viruses were quantified by qPCR, applied to DNase I-pretreated culture media (to eliminate unencapsidated DNA). Data are presented as average genome titers from biological triplicates, with individual data points and standard deviations shown; Student's t-test-calculated *P* values (unpaired; two-tailed) for STS^X and TWR^X viruses relative to the WT virus were 0.0025 and 0.0001, respectively.

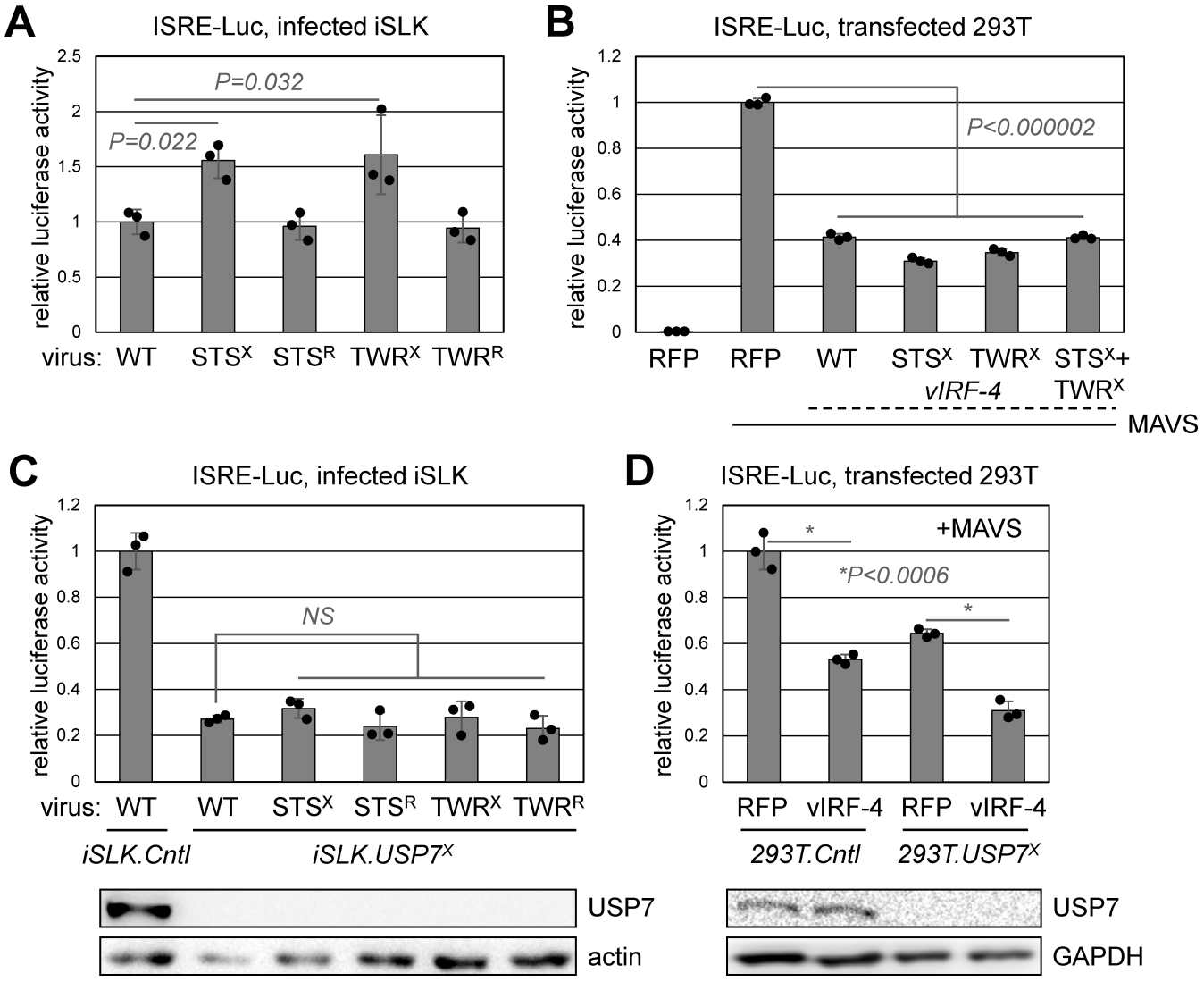

FIG 2 Assessment of innate-immune signaling as a function of vIRF-4–USP7 interaction. (A) HHV-8 BAC16-infected iSLK cultures were transfected with an ISRE-regulated luciferase reporter (ISRE-Luc), and lytic reactivation was induced by Dox/NaB treatment for 1 day prior to cell harvest for luciferase assays. Triplicate cultures of each type were analyzed, and average luciferase activities, relative to that for WT-virus-infected cells, are presented. Student's *t*-test *P* values (two-tailed) for STS^X and TWR^X viruses relative to WT are shown; average values for repaired viruses (STS^R; TWR^R) were very similar to that for the native (WT) virus, as expected. (B) Transfection-based ISRE-Luc reporter assays using 293T cells expressing WT or mutated vIRF-4 or red fluorescent protein (RFP) control and IFN-I-inducing MAVS. Luciferase activities were determined after 1 day, from biological triplicates; average values are shown, relative to that from RFP/MAVS cultures. WT- vs mutant-vIRF-4 values were significantly (Student's *t*-test *P* values 0.008 and 0.005, respectively) but not substantially reduced for STS^X and TWR^X, but not significant for STS^X+TWR^X. (C) ISRE-Luc reporter assays were carried out using infected iSLK cells deleted of USP7 (iSLK.$USP7^X$) via lentiviral vector-mediated Cas9/gRNA transduction (see Materials and Methods); control iSLK cells (iSLK.Cntl) were transduced with a vector expressing a nontargeting gRNA along with Cas9. Luciferase activities from triplicate cultures were determined after 1 day of Dox/NaB treatment to induce lytic replication. Differences in luciferase activities between WT and mutated vIRF-4 samples in iSLK.$USP7^X$ cells were statistically not significant (NS). Culture samples were immunoblotted to show USP7 ablation in iSLK.$USP7^X$ cells. (D) ISRE-Luc reporter assays were carried out in control and USP7-deleted 293T cells to test the influence of USP7 on vIRF-4 suppression of MAVS/IFN-I-activated signaling. Significant suppression of ISRE-Luc activity by vIRF-4 was evident in both the presence and absence of USP7, as determined by Student's *t*-test (two-tailed). USP7 deletion caused a significant reduction of reporter activity ($P < 0.002$ for RFP and vIRF-4, 293T.Cntl vs 293T.$USP7^X$).

vIRF-4-overexpressing transfected cells, or perhaps be dependent on the cell type or mechanisms specific to infected cells (by virtue of other viral proteins or modulated cellular factors).

To test the involvement of USP7 in the mutation effects observed in infected cells, we carried out equivalent reporter experiments using USP7-ablated iSLK cells (iSLK.USP7^X) (see Materials and Methods). In this context, the mutations had an insignificant impact on ISRE-luciferase reporter activity (Fig. 2C), indicating an important role of USP7 in the observed functional effects of the mutations in native iSLK cells. In transfected WT–control (Cas9$^+$/non-targeting-gRNA$^+$) and USP7-ablated 293T cells, ISRE-reporter activity was suppressed by vIRF-4, demonstrating USP7-independent activity of vIRF-4 (Fig. 2D). However, luciferase activity was generally lower in USP7-deficient cells, revealing a positive role of USP7 in overall ISRE-activating signaling. This was also evident in lytically reactivated iSLK.USP7^X cells in comparison to control iSLK (Cas9$^+$/nontargeting-gRNA$^+$) cells (Fig. 2C). Together, our data demonstrate the significance of targeting of USP7 by vIRF-4 with respect to suppression of antiviral signaling in infected iSLK cells, likely contributing to the pro-replication activity of vIRF-4 via its interaction with USP7, and a direct role of vIRF-4 in suppression of such signaling, as evidenced in transfected 293T cells.

USP7 regulation of vIRF-4 ubiquitination and expression

That USP7 binds vIRF-4 raises the possibility that vIRF-4 itself is a substrate of the deubiquitinase and is potentially subject to enhanced expression via salvage from ubiquitin-promoted degradation (25, 26). To examine this possibility, we first assessed ubiquitination of Flag-tagged vIRF-4 and USP7-binding-deficient STS^X and TWR^X variants, in addition to a variant containing both mutations (STS^X+TWR^X or S^X+T^X), in transfected 293T cells. To facilitate detection of ubiquitin-modified vIRF-4 proteins, the cells were cotransfected with a ubiquitin expression plasmid. Immunoblot analysis of the Flag-antibody-precipitated (denatured) protein from the respective cell lysates identified vIRF-4 polyubiquitination, both general and specifically K48-linked, that was increased for the mutated proteins relative to wild-type vIRF-4, with double-mutated vIRF-4 showing the greatest level of ubiquitination (Fig. 3A). The data suggest first that vIRF-4 is a substrate of bound USP7 and second that vIRF-4 may be subject to ubiquitin-directed proteasomal degradation. The former was supported via equivalent analyses in USP7-ablated 293T cells, in which the positive effects of the vIRF-4 mutations on vIRF-4 ubiquitination were abolished (Fig. 3B).

Similar analyses were carried out on iSLK cells infected with BAC16-based recombinant viruses expressing 3xFlag-tagged vIRF-4, vIRF-4.STS^X, or vIRF-4.TWR^X. Flag-immunoprecipitations from day-2 lytic-cell lysates and immunoblotting identified increased overall and K48-linked ubiquitination of the vIRF-4 variants relative to wild-type vIRF-4 (Fig. 3C). A similar experiment utilizing control (iSLK.Cntl) and USP7-ablated (iSLK.USP7^X) cells confirmed the role of USP7 in regulating vIRF-4 ubiquitination via direct interaction with vIRF-4 (Fig. 3D). In this experiment, USP7 ablation did not lead to an overall increase in vIRF-4 ubiquitination, as expected; the reason for this is likely to relate to indirect effects of USP7 loss on other cellular processes impacting vIRF-4 ubiquitination levels. Regardless of this, the data show that vIRF-4, in isolation in transfected cells and in HHV-8-infected cells, is subject to ubiquitination that can be suppressed (presumably via deubiquitination) by vIRF-4-bound USP7.

Although the ubiquitination data from transfected and infected cells are concordant, the vIRF-4 mutations enhanced ISRE-reporter activity only in the latter (Fig. 2A and B), possibly due to overexpression and consequent loss of ubiquitin-directed regulation of vIRF-4 in transfected cells. Thus, using immunoblotting, we examined whether the STS^X and TWR^X mutations affected vIRF-4 expression in infected cells, utilizing viruses expressing the 3xFlag-tagged versions of these and wild-type vIRF-4 proteins. In cells harvested on day 2 following lytic reactivation of the respective viruses from infected iSLK cells, we saw reduced expression of the vIRF-4 variants (Fig. 3E). Other detected lytic proteins (vIRF-1 and vIL-6) were also suppressed by the vIRF-4 mutations, likely resulting from increased innate-immune signaling (Fig. 2) and other vIRF-4-regulated antiviral and/or transcriptional mechanisms (10–12, 27). To examine the expression of vIRF-4,

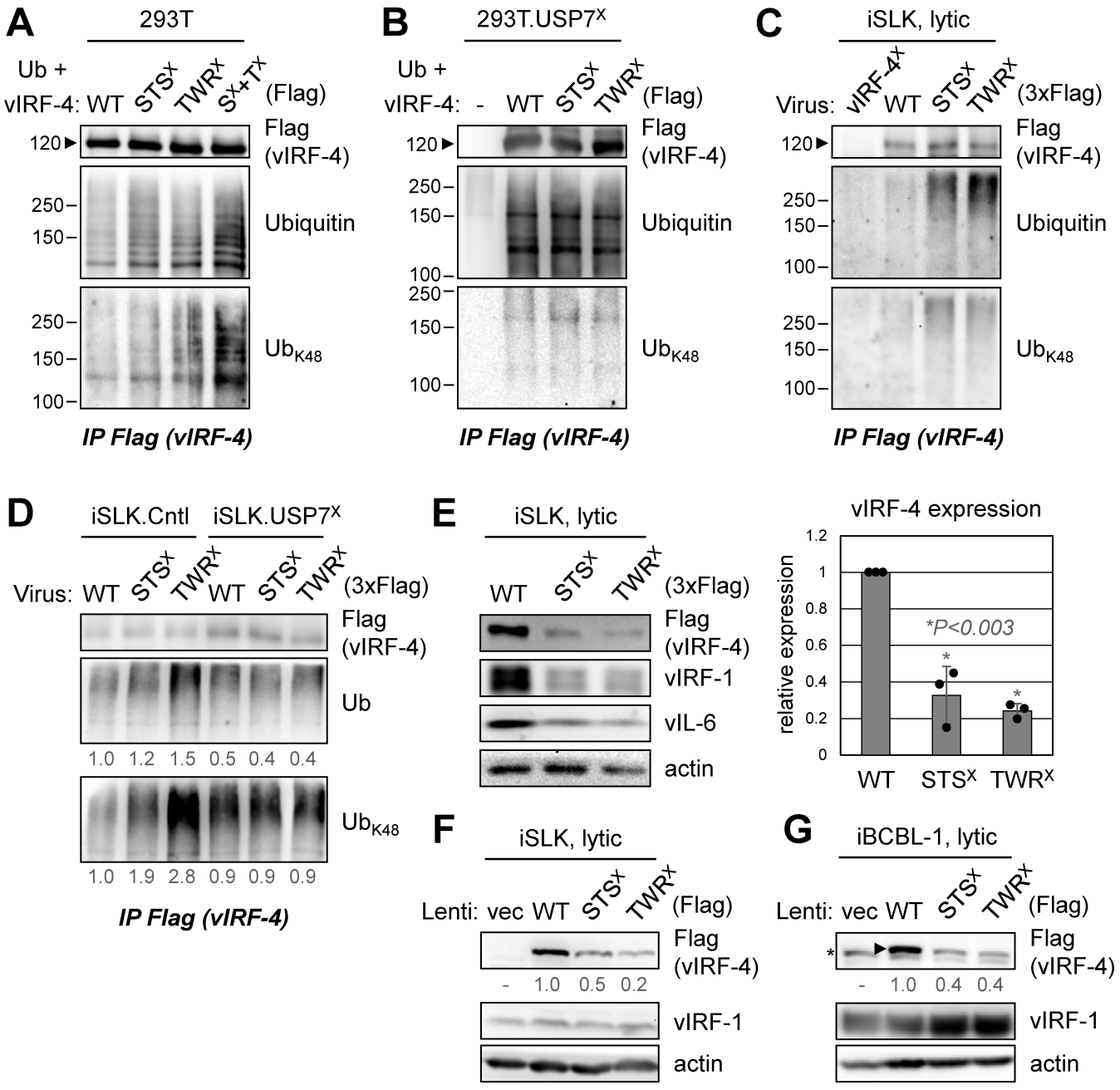

FIG 3 Regulation of vIRF-4 ubiquitination and expression via USP7 binding. (A) Immunoprecipitation (IP)-based analysis of vIRF-4 ubiquitination in transfected 293T cells. Cells were transfected with expression vectors for Flag-tagged vIRF-4 (WT), vIRF-4.STS^X, vIRF-4.TWR^X, or vIRF-4.STS^X+TWR^X (S^X+T^X) along with a ubiquitin (Ub) expression vector. Proteins were precipitated from denatured cell lysates with Flag antibody-beads, and the precipitated protein was then analyzed by immunoblotting for ubiquitin (total) and K48-linked polyubiquitin (Ub$_{K48}$). The apparent size of vIRF-4-Flag is indicated (arrowhead). (B) An equivalent analysis of vIRF-4 ubiquitination was carried out in USP7-ablated 293T cells (293T.USP7^X). (C) Ubiquitination of 3xFlag-tagged vIRF-4, vIRF-4.STS^X, and vIRF-4.TWR^X was assessed in iSLK cells infected with the respective BAC16 recombinant viruses and treated for 2 days with Dox/NaB to induce lytic replication. Flag-immunobead-precipitated vIRF-4–3xFlag proteins were immunoblotted for detection of total-ubiquitin and K48-linked–ubiquitin conjugates. Virus ablated of vIRF-4 (vIRF-4^X) was used to verify lack of an appreciable background signal. (D) A similar analysis was carried out using USP7-ablated iSLK cells (iSLK.USP7^X), along with control (Cas9$^+$/non-targeting-gRNA$^+$) iSLK cells (iSLK.Cntl). Levels of total-ubiquitin (Ub) and K48-linked–ubiquitin (Ub$_{K48}$) conjugates relative to those of WT vIRF-4 in iSLK.Cntl cells, and normalized to precipitated vIRF-4, are indicated below each ubiquitin blot. (E) Assessment of the relative expression of Flag-tagged vIRF-4, vIRF4.STS^X, and vIRF-4.TWR^X in Dox/NaB-treated iSLK cells infected with the respective viruses. Cell lysates after 2 days of lytic induction were analyzed by immunoblotting for vIRF-4 (Flag) in addition to vIRF-1, vIL-6, and β-actin. Levels of mutated vIRF-4 relative to WT vIRF-4, normalized to β-actin, from triplicate samples are shown in the chart. Statistical significance was determined by Student's *t*-test. (F) A similar experiment was carried out using

(Continued on next page)

FIG 3 (Continued)

vIRF-4-Flag-expressing lentivirus vector-transduced WT-HHV-8$^+$ iSLK cells. Levels of mutated relative to wild-type vIRF-4-Flag, normalized to β-actin, are shown below the Flag blot. vec, empty lentivirus vector. (G) Analogous assessments of the expression of WT and USP7-binding-refractory vIRF-4 proteins in lentiviral vector-transduced iBCBL-1 (TRExBCBL1-RTA) PEL cells. *, nonspecific band; arrowhead, vIRF-4 band.

vIRF-4.STS^{X,} and vIRF-4.TWR^X independently of other effects, the proteins were introduced into wild-type-HHV-8$^+$ iSLK cells via lentiviral vector transduction prior to lytic induction and cell harvest after 2 days. Levels of the lentiviral vector-derived Flag-tagged vIRF-4 variants were reduced relative to those of native vIRF-4-Flag, without vIRF-1 expression being affected (Fig. 3F). A similar experiment was carried out using Dox-inducible TRExBCBL1-RTA PEL cells (24) (here referred to as iBCBL-1 cells), in which each of the vIRF-4 mutations led to reduced vIRF-4, but not vIRF-1, expression (Fig. 3G). Overall, these data suggest that targeting of USP7 by vIRF-4 is important for its expression, likely resulting from USP7-mediated deubiquitination of vIRF-4 and consequent rescue from proteasomal degradation.

Virus replication as a function of vIRF-4 expression

To examine the overall role of vIRF-4 in HHV-8 replication, and thereby test the hypothesis that ubiquitin- and USP7-mediated regulation of vIRF-4 can modulate productive replication, we examined the effect of vIRF-4 depletion. First, three shRNAs directed to vIRF-4 mRNA were tested in transfected cells for vIRF-4 depletion efficacy; shRNAs 2 and 3 were found to be highly effective (Fig. 4A). Lentiviral vectors expressing these shRNAs, or non-silencing (ns) control shRNA, were used to transduce separate iSLK cultures, which were then infected with HHV-8 and subsequently treated with Dox/NaB to induce lytic replication. Encapsidated (DNase I-resistant) viral genomes released into the culture media over 6 days were quantified by qPCR, revealing greatly reduced virus production in vIRF-4-depleted cells (Fig. 4B). In iBCBL-1 cells, in which vIRF-4-specific shRNA-2 was demonstrated to suppress vIRF-4 mRNA (Fig. 4C), a similar effect was observed on virus production (Fig. 4D).

To verify the importance of vIRF-4 for HHV-8 productive replication, we used BAC16-based recombineering to knock out vIRF-4, changing the translation–initiator-ATG codon to TTG; the mutation was verified by sequencing, and the overall genome integrity was checked by restriction digestion (Fig. 4E). Cultures of iSLK cells were infected with equal infectious doses of WT and vIRF-4-null (vIRF-4^X) viruses, and equivalent LANA expression was confirmed by immunoblotting (Fig. 4F). Comparisons of virus production from the respective Dox/NaB-treated cultures revealed dramatic suppression of released encapsidated viral genomes as a consequence of vIRF-4 ablation (Fig. 4G). This was reflected in significantly reduced expression of early and late transcripts from ORFs 24 and K8.1, respectively (Fig. 4H). Interestingly, levels of vIRF-1 mRNA, induced directly by RTA (28, 29), were increased as a result of vIRF-4 ablation, despite reported positive regulation of vIRF-1 transcription by vIRF-4 via cooperative functional interaction with RTA (12). Increased expression of vIRF-1 mRNA in the context of vIRF-4 knockout contrasts with the effect of USP7-binding ablation on vIRF-1 protein expression (Fig. 3E); determining the underlying mechanisms will require further, in-depth investigation.

Regulation of antiviral signaling by vIRF-4

To investigate IFN-I signaling suppression by vIRF-4 in the context of lytic replication, we utilized our ISRE-Luc reporter in Dox/NaB-treated iSLK cells infected with wild-type or vIRF-4-ablated (vIRF-4^X) HHV-8. Luciferase activity was increased significantly in the absence of vIRF-4 (Fig. 5A). RT-qPCR analyses of selected IFN-I-induced genes, IFN-α1 and IFN-β1, in lytically infected cells demonstrated the induction of the former as a result of vIRF-4 ablation (Fig. 5B), generally consistent with the reporter data. Depletion of vIRF-4 in Dox-treated iBCBL-1 cells yielded essentially the same result (Fig. 5C). Thus, vIRF-4 is able to inhibit induction of IFN-I gene expression and downstream signaling in the

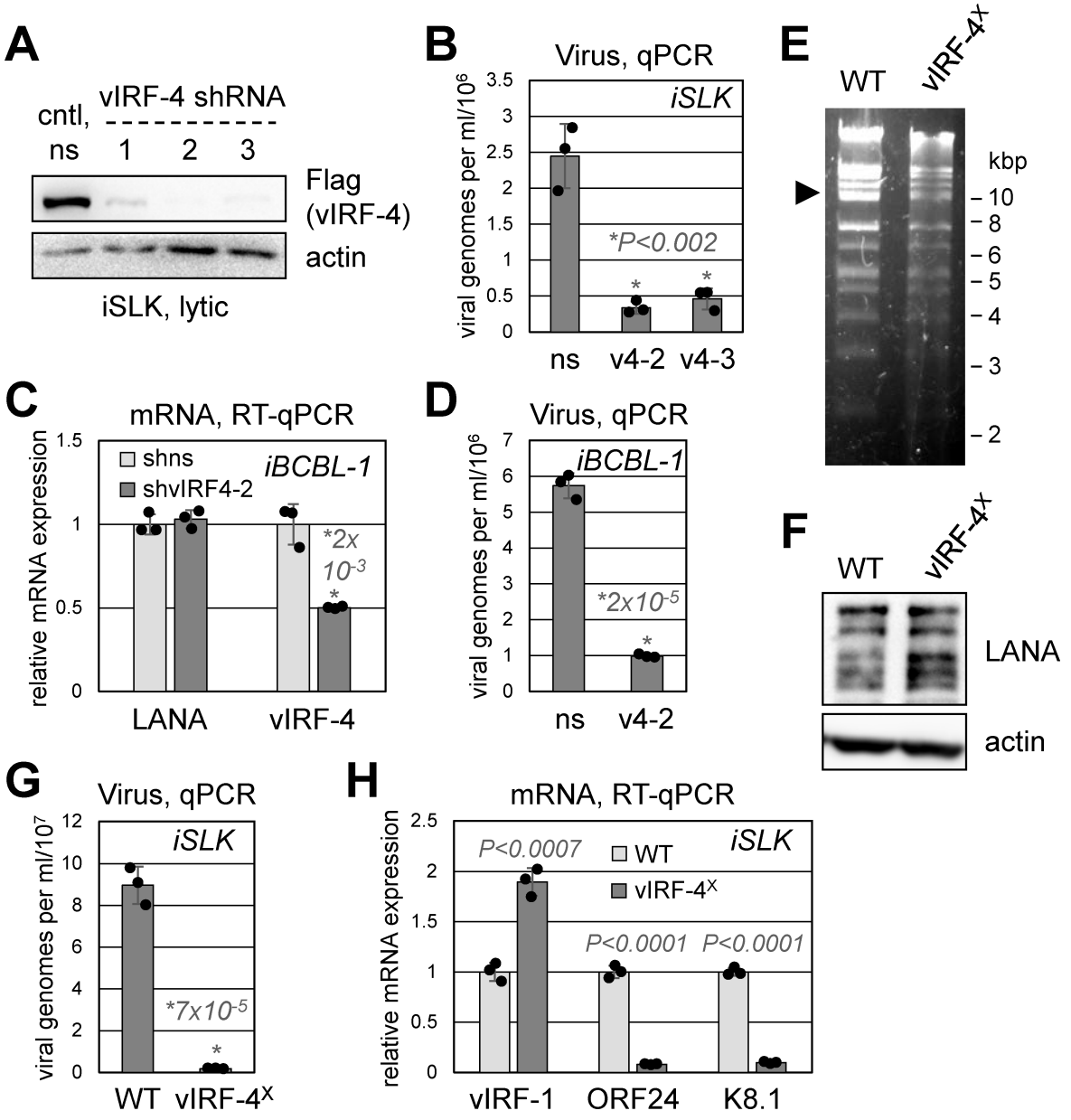

FIG 4 Contribution of vIRF-4 to HHV-8 productive replication. (A) Testing efficacies of vIRF-4 mRNA-directed shRNAs. Lentiviral vectors expressing each of three vIRF-4-specific shRNAs, or non-silencing (ns) control shRNA, were used to infect BAC16.vIRF-4.3xFlag^{+} iSLK cells, which were subsequently treated with Dox/NaB to induce lytic replication and vIRF-4 expression. Cells were harvested 48 h post-induction, and lysates were analyzed by Flag-immunoblotting for vIRF-4 levels. (B) Virus productive replication in iSLK cells as a function of vIRF-4 depletion via shRNA (v4-2; v4-3) was determined by qPCR analysis of encapsidated (DNase I-resistant) viral genomes released into culture media during 6 days of lytic induction with Dox/NaB treatment. Data are presented as average values from triplicate cultures. Student's *t*-test *P* values are indicated (ns vs vIRF-4 shRNAs). (C) Testing of vIRF-4 shRNA (shvIRF4-2) efficacy in lentiviral vector-transduced iBCBL-1 cells, treated with Dox to induce lytic replication. Cells were harvested 24 h after induction for RNA extraction and RT-qPCR analyses of LANA (negative control) and vIRF-4 mRNA levels in vIRF-4 relative to control (ns) shRNA-expressing cells. Triplicate cultures were analyzed, and averages are shown, along with the *P* value (*) for vIRF-4 mRNA depletion. (D) Virus production from vIRF-4-depleted (v4-2) versus control (ns) iBCBL-1 cells treated for 48 h with Dox to induce lytic replication. Data were derived from triplicate cultures; average qPCR-determined genome titers are shown. (E) Restriction (SpeI) analysis of WT and vIRF-4-knockout (vIRF-4^{X}) BAC16 genomes; the latter contains mutation of the translation–initiator ATG codon to TTG. The arrowhead indicates the position of the band containing vIRF-4 coding sequences. (F) LANA immunoblotting of infected iSLK-cell lysates, verifying equivalent expression and viral loads for WT and vIRF-4-knockout virus-infected cultures. (G) Virus production in WT and vIRF-4^{X} virus-infected iSLK cells, as measured by qPCR applied to encapsidated (DNase I-resistant) viral genomes released into the media during 6 days of Dox/NaB treatment. Data from biological triplicates are expressed as averages. (H) RT-qPCR analysis of selected early (vIRF-1; ORF24) and late (K8.1) viral gene transcripts in wild-type and vIRF-4-knockout (vIRF-4^{X}) virus-infected and Dox/NaB-treated

(Continued on next page)

FIG 4 (Continued)

iSLK cells, harvested 48 h after lytic induction. Transcript levels, normalized to GAPDH mRNA, from triplicate cultures are shown relative to average levels in WT virus-infected cells. Student's *t*-test *P* values are shown for vIRF-4-knockout-effected changes in transcript levels.

context of lytically infected cells, likely accounting in part for the pro-replication activity of vIRF-4.

Interestingly, vIRF-4 knockout or depletion in iSLK and iBCBL-1 cells did not substantially affect the levels of p53 (Fig. S2), in contrast to previously reported suppression of p53 by overexpressed vIRF-4 and speculated associated function of vIRF-4 (16, 27). The levels of p53 were also essentially unaffected by the STS^X and TWR^X mutation-effected disruption vIRF-4 interaction with USP7 (Fig. S2A).

vIRF-4–USP7 interaction in TRAF3 regulation

It has been reported that vIRF-4 can suppress interferon expression via an inhibitory interaction with transcription factor IRF7 (7). As outlined above, we found that MAVS-stimulated signaling, initiated via TRAF3 and TRAF6 E3 ubiquitin ligases and activating IRF3/7 and IFN-I-responsive ISRE reporters, is inhibited by vIRF-4 (Fig. 2B and D). Therefore, we assessed the effect of vIRF-4, and its interaction with USP7, on upstream TRAF3 polyubiquitination, effecting activation via K_{63}-linkage (30). This was examined first in transfected cells, in the presence of overexpressed TRAF3 and ubiquitin. Coexpression of wild-type vIRF-4 suppressed auto-ubiquitination of TRAF3 (Fig. 6A). However, the STS^X and TWR^X mutations had no detectable effect on vIRF-4 inhibition of TRAF3 ubiquitination, indicating that the vIRF-4–USP7 interaction, in contrast to that between vIRF-2 and USP7 (15), does not affect TRAF3 activity. Indeed, vIRF-4 suppression of TRAF3 polyubiquitination was retained in USP7-knockout cells (Fig. 6B), demonstrating a USP7-independent mechanism of TRAF3 inhibition by vIRF-4.

Similar IP-based analyses of TRAF3 ubiquitination were carried out in TRAF3-S-expressing (lentiviral vector-transduced) iSLK cells infected with wild-type, vIRF-4.STS^X- or vIRF-4.TWR^X-expressing, wild-type-reverted (STS^R; TWR^R), or vIRF-4-null (vIRF-4^X) BAC16 viruses. In contrast to the results in transfected cells (Fig. 6A), TRAF3 ubiquitination was detectably increased as a function of the introduced STS^X and TWR^X mutations (Fig. 6C).

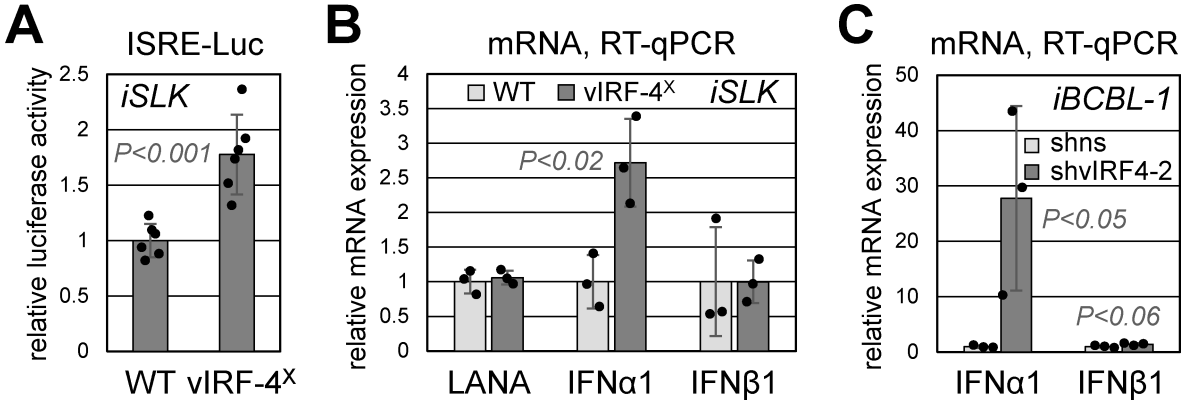

FIG 5 Influence of vIRF-4 on the IFN pathway. (A) ISRE-Luc reporter-determined influence of vIRF-4 on IFN-I signaling, utilizing reporter-transfected iSLK cells infected with WT or vIRF-4-knockout (vIRF-4^X) HHV-8. Cultures were treated for 30 h with Dox/NaB to induce lytic replication prior to cell harvest and determinations of luciferase activity. Activities from six biological replicates were determined, and relative individual and average values (WT average set at 1) are shown along with standard deviations and Student's t-test-derived *P* value. (B) RT-qPCR determinations of relative levels of selected IFN-I genes, IFN-α1 and IFN-β1, in WT and vIRF-4^X virus-infected and lytically induced iSLK cultures (triplicates). Cultures were treated for 48 h with Dox/NaB before cell harvest and RNA extraction. The IFN-I transcripts and LANA mRNA levels were normalized to GAPDH mRNA, and average values relative to levels in WT-virus-infected cells are shown. The change in the IFN-α1 level as a result of vIRF-4 ablation was statistically significant (Student's *t*-test). (C) A similar experiment was carried out using iBCBL-1 cells, transduced with either control shRNA (shns) or vIRF-4 mRNA-targeted shRNA (shvIRF4-2) prior to lytic induction with Dox. Cells were harvested after 24 h of Dox treatment.

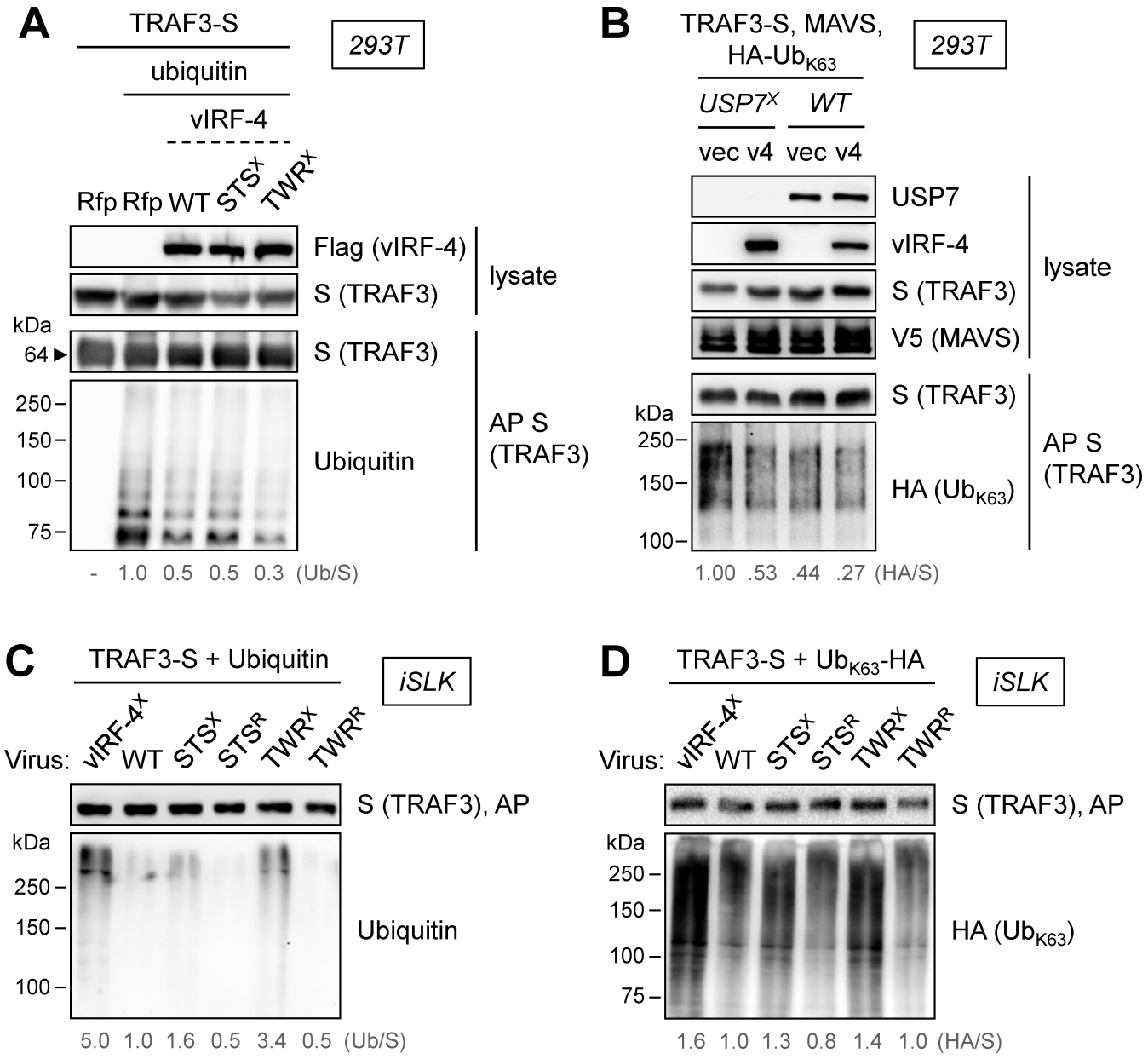

FIG 6 Regulation of TRAF3 ubiquitination by vIRF-4. (A) Expression vectors expressing S-tagged TRAF3, vIRF-4 (WT or mutated) or RFP (control), and ubiquitin were transfected into 293T cells, and denatured cell lysates were subsequently generated and used for affinity precipitation (AP) of TRAF3-S, which was analyzed by immunoblotting for ubiquitin. (B) Analogous AP analysis of TRAF3 K63-linked ubiquitination in USP7-knockout ($USP7^X$) 293T cells in comparison to wild-type (WT, control-gRNA$^+$/Cas9$^+$) cells. In this experiment, vectors expressing HA-tagged K63-only ubiquitin (Ub_{K63}) and TRAF3-activating MAVS were cotransfected. vec, empty vector; v4, vIRF-4. (C) A similar experiment to detect TRAF3 ubiquitination was carried out using iSLK cells infected with WT, vIRF-4.STS^X, vIRF4-.TWR^X, repaired (STS^R; TWR^R), or vIRF-4^X HHV-8 and lytically induced by Dox/NaB treatment for 48 h before cell lysis and TRAF3-S AP. TRAF3-S and ubiquitin were introduced via lentiviral vector transduction. (D) An analogous experiment was carried out using lentivirally expressed HA-tagged K63-only ubiquitin (Ub_{K63}).

Increased TRAF3 ubiquitination was observed also in response to vIRF-4 knockout, indicating that the effects via mutation of the USP7-binding motifs can be accounted for by regulation of vIRF-4 expression. Specific probing for TRAF3-activating K63-linked polyubiquitination, via introduction of K63-only HA-tagged ubiquitin, yielded similar results (Fig. 6D), demonstrating that vIRF-4 can inhibit TRAF3 activity and that binding of USP7 by virus-expressed vIRF-4 influences this, likely via promotion of vIRF-4 expression (Fig. 3).

TRAF3 is a regulator of HHV-8 replication

The functional significance of TRAF3 to HHV-8 productive replication was assessed via its depletion in iSLK and iBCBL-1 cells. Several tested, lentiviral vector-delivered shRNAs were ineffective, leading to the use of TRAF3-directed gRNA, or nontargeting control, expressed along with Cas9 to knockout TRAF3 alleles. This approach was sufficient to achieve knockdown of TRAF3 within the overall, mixed cultures of lentiviral vector-transduced cells (Fig. 7A and B). Depletion of TRAF3 in the HHV-8$^+$ iSLK and iBCBL-1 cultures led to substantially increased virus yields from each culture after lytic reactivation (Fig. 7C and D). These data demonstrate the suppressive effect of TRAF3 on lytic replication in both cell types, indicating that inhibition of TRAF3 by vIRF-4 is a significant mechanism of pro-viral activity by the viral protein.

DISCUSSION

The presented data have identified ubiquitination of vIRF-4, positive regulation of vIRF-4 via its interaction with USP7, suppression of TRAF3 activity and antiviral signaling by vIRF-4, and the importance of such vIRF-4 activity for HHV-8 productive replication. It has been reported that vIRF-4 depletion suppresses HHV-8 replication in the context of iSLK cells, correlating with the identified role of vIRF-4 in transcription from its own and other viral lytic promoters and with manipulation of cellular gene expression (11,

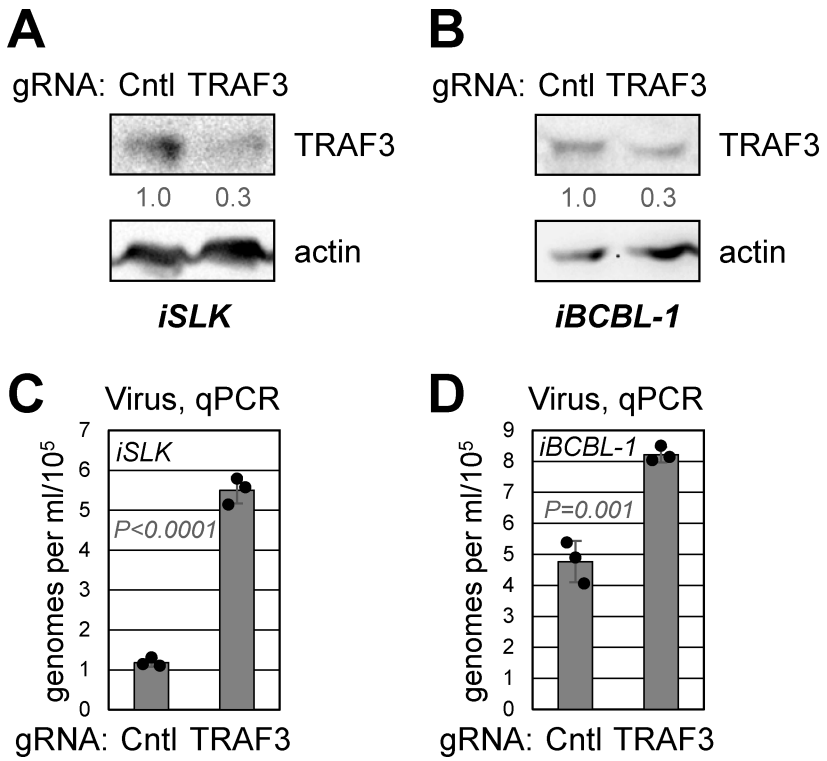

FIG 7 Contribution of TRAF3 to regulation of HHV-8 productive replication. (A, B) Lentiviral vector-delivered Cas9 and TRAF3 gene-directed gRNA were used to effect TRAF3-gene knockout and overall depletion of TRAF3 in HHV-8$^+$ iSLK and iBCBL-1 cultures. A vector expressing nontargeting gRNA along with Cas9 was used as a control (Cntl). Cell lysates from iSLK (A) and iBCBL-1 (B) cultures were analyzed by immunoblotting to assess TRAF3 depletion; relative, actin-normalized levels are shown below the TRAF3 blots. (C, D) The iSLK and iBCBL-1 cultures were induced into lytic replication by treatment with Dox/NaB and Dox, respectively, and the culture media from biological triplicates were collected over the course of 6 days (iSLK) or 2 days (iBCBL-1). DNase I-resistant (encapsidated) viral genomes in the respective culture media were quantified by qPCR; average yields from the iSLK (C) and iBCBL-1 (D) cultures are shown, along with Student's t-test-derived *P* values.

12). Here, we have verified, via direct genetic ablation in addition to depletion of vIRF-4, the importance of vIRF-4 to HHV-8 replication in iSLK and also PEL cells and, moreover, have shown the specific importance of interaction of vIRF-4 with USP7. The suppression of K63-polyubiquitinated (active) TRAF3 and downstream interferon signaling by vIRF-4 is likely to contribute to its positive regulation of productive replication. Indeed, TRAF3 depletion led to significantly increased virus production in both iSLK and iBCBL-1 cells. Of note, the suppression of TRAF3 activity and interferon signaling by vIRF-4 was contrary to the corresponding positive (and counterintuitive) activities of vIRF-2 that we reported previously (15). It is likely that a balance of such signaling is important for overall viral replication and fitness in the host, if not in the culture, for example, by limiting the host adaptive immune response to infection through restriction of virus production and antigen expression.

Previously reported activities of vIRF-4 include its targeting and stabilization of the E3 ubiquitin ligase MDM2, which leads to inhibition of auto-ubiquitination and thereby rescue of the enzyme from K48-polyubiquitination-promoted proteasomal degradation (27). As p53 is a substrate of MDM2, inhibitory targeting and stabilization of the enzyme lead to the promotion of p53 degradation and suppression of associated pro-apoptotic and antiviral signaling. This certainly has the potential to contribute to the pro-replicative activity of vIRF-4 reported in iSLK cells (12). However, we did not detect increases in p53 levels in response to vIRF-4 knockout or depletion in iSLK and iBCBL-1 cells nor in response to mutation-effected disruption of vIRF-4–USP7 interaction in infected iSLK cells, suggesting that p53 regulation by vIRF-4 via its interaction with USP7 or otherwise may not be a significant contributor to vIRF-4 function. Of relevance to potential p53 regulation by vIRF-4 is the reported inhibitory targeting by vIRF-4 of USP7 (16), which can deubiquitinate p53 and lead to its stabilization. Viral IRF-4-derived peptides containing USP7-interacting sequences were found to effect USP7 inactivation and loss of PEL-cell viability in culture and in engrafted mice (16). However, as noted in this report, the significance of a full-length vIRF-4 interaction with USP7 remained open to question. In view of USP7-depletion-induced loss of lytically infected PEL cell viability and HHV-8 productive replication therein (14), it seems unlikely that virus-expressed vIRF-4 acts to block USP7 activity. Indeed, we have found that vIRF-4 polyubiquitination is suppressed and vIRF-4 expression enhanced in a USP7-binding-dependent manner, suggesting productive engagement of the deubiquitinase by vIRF-4. As vIRF-4 has been shown previously (12) and in this study to be required for efficient virus replication, our data suggest that enhanced vIRF-4 expression via its interaction with USP7 is biologically important.

Our finding of TRAF3 inhibition by vIRF-4 provides new information about innate-immune signaling suppression by the viral protein. While this could occur independently of USP7–vIRF-4 interaction, we cannot, on the basis of the presented data, rule out the possibility that USP7-mediated mechanisms may also be involved. Of relevance to innate-immune signaling regulation by vIRF-4 are previously reported biotin proximity labeling-based screening data identifying various proteins, including the mRNA splicing factors SF3B1 and SNW1, as potential interaction partners of vIRF-4 (as well as vIRF-1), with the former confirmed in a coprecipitation assay (31). Depletion of either of these cellular factors led to reduced expression of poly(I:C)/RIG-I-induced IFN-β1 and IFN-λ1 mRNA in 293T cells and lytic replication-induced IFN-α1 and IFN-β1 mRNA in addition to viral transcripts and HHV-8 production in infected iSLK cells. Thus, targeting of the splicing factors by vIRFs 1 and 4 could influence replication-suppressing interferon expression. Overexpression of the vIRFs in 293T cells led to reduced levels of IFN-I α1 and β1 mRNAs induced by RIG-I signaling. Another report identified the inhibitory interaction of vIRF-4 with IRF7, with consequent suppression of Sendai virus-induced IFN-α1, -α4, and -α6 in 293T cells (7). Our identification via experimental use of vIRF-4-ablated HHV-8 of vIRF-4 suppression of IFN-α1 transcripts in lytically infected iSLK cells is in general agreement with these previous findings, although IFN-β1 transcripts were not detectably affected by vIRF-4 knockout. We found that IFN-α1 gene expression was suppressed

by vIRF-4 also in lytically infected iBCBL-1 cells, as vIRF-4 depletion increased IFN-α1 mRNA levels. Our finding in transfected 293T cells that vIRF-4 could inhibit IFN-β-induced ISRE-responsive reporter activity was also significant and to our knowledge is the first report of IFN-I-signaling inhibition by vIRF-4.

With respect to vIRF-4 activity in HHV-8 replication, it has been reported that vIRF-4 cooperates with the viral immediate–early replication and transcriptional activator, RTA, to promote expression of its own and other early lytic genes (12). Also, vIRF-4, through targeting of β-catenin/CBP, effects repression of cyclin D1 and consequent G1-S cell-cycle arrest and, as identified by vIRF-4 overexpression, promotion of virus lytic replication in iBCBL-1 cells (11). Our present studies, employing recombinant viruses ablated of vIRF-4 or expressing USP7-refractory vIRF-4 in iSLK cells, depletion of vIRF-4 in both iSLK and iBCBL-1 cells, and analysis of viral vector-expressed native and USP7-binding-deficient vIRF-4 proteins in iSLK and iBCBL-1 cells, verify the importance of vIRF-4 and its interaction with USP7 for productive replication in both cell types. While potential mechanisms of vIRF-4 pro-replication activity via USP7 interaction have not been determined, we have identified the importance of the interaction for expression of vIRF-4 itself, which, as outlined, can function in different ways to promote lytic replication.

In conclusion, we have confirmed a critical role of vIRF-4 in HHV-8 productive replication, for the first time using genetic ablation of the vIRF-4 ORF within the viral genome, and determined the importance of vIRF-4–USP7 interaction for this activity; identified USP7-binding-restricted K48-linked polyubiquitination of vIRF-4 and the role of USP7 interaction in vIRF-4 expression; and determined the importance of TRAF3 in suppression of HHV-8 lytic replication and a role of vIRF-4 in inhibiting TRAF3-mediated innate-immune signaling, accounting in part for the pro-replication activity of vIRF-4. These findings contribute significantly to our understanding of factors regulating vIRF-4 expression and mechanisms of vIRF-4 innate-immune evasion and pro-viral activity.

MATERIALS AND METHODS

Cell culture and transfections

HEK293T and iSLK cells (24) were cultured in Dulbecco's modified Eagle medium (DMEM), and TREx BCBL1-RTA (or "iBCBL-1") cells (32) were cultured in RPM-1640 medium; media were supplemented with 10% fetal bovine serum (FBS), gentamycin (10 µg/mL), and plasmocin (2.5 µg/mL). USP7-knockout 293T and iSLK cells were engineered via Cas9 and gRNA co-expressing lentiviral vector transduction and selection in blasticidin (10 ng/mL) for ~10 days prior to experimental use. DNA transfections into ~70%-confluent 293T cells were carried out using mixtures of plasmid DNA and linear cationic polymer polyethylenimine (Polysciences, catalog number: 593215). Mixtures of Lipofectamine 2000 (Thermo Fisher, 11668030) and plasmid DNA were used for transfections of iSLK cells; culture DMEM was replaced with Opti-MEM (Gibco, 31985062) prior to addition of DNA/Lipofectamine. After at least 6 h, transfection media were replaced with supplement-containing DMEM. Cells were harvested ~48 h post-transfection for immuno/affinity-precipitation and/or immunoblotting, and luciferase assays were performed after ~24 h of further incubation of cultures at 37°C.

Plasmids and oligonucleotides

The following plasmids used in the present study were reported previously: USP7-CBD expression vector pCEBZ-USP7-CBD (14); lentiCRISPRv2-blast vectors (Addgene 98293; deposited by Dr. B. Stringer) expressing USP7-specific gRNA or nontargeting control RNA along with Cas9 (33); MAVS expression vector pICE-V5-MAVS (34); reporter plasmid pISRE-Luc (35); RFP expression plasmid pCEBZ-RFP-CBD (36); pRK5-based expression vectors for HA-tagged wild-type and K63-only ubiquitin (37) (Addgene 17608 and 17606; deposited by Dr T. Dawson); pCEBZ-TRAF3-S (15). pRL-TK, expressing Renilla luciferase constitutively, was obtained from Promega (E2241). The vIRF-4 open-reading frame (ORF) was PCR-amplified from BAC16 using appropriate primers flanked by NotI

and XhoI restriction enzyme sites and cloned between these sites in pCEBZ-RFP-CBD, replacing RFP ORF sequences. STS^X and TWR^X mutations (to amino acid residues AAA, new codons GCA-GCA-GCA) were introduced into the vIRF-4 ORF using overlapping PCR, and the respective ORFs were cloned into pCEBZ-RFP-CBD. Vectors expressing shRNAs were generated by cloning of ds-DNA oligonucleotides into the lentivirus vector plasmid pYNC352, using BamHI and MluI cloning sites. A vector expressing non-silencing (NS) control shRNA was described previously (38). Equivalent vectors were generated to express shRNAs targeting vIRF-4 mRNA sequences GCCCAGAGTTCCACTT GTTAG (shvIRF4-1), GGTGGTAGCTACGTAGTATGG (shvIRF4-2), and GGATACAGACGCGTGA CAACT (shvIRF4-3). A double-stranded oligonucleotide specifying TRAF3-gene-directed gRNA (target sequence AGCCCGAAGCAGACCGAGTG; gTRAF3-4) was cloned between the doublet BsmBI cloning sites of lentiCRISPRv2-blast. Primers used for qPCR of reverse-transcribed RNAs were as follows: LANA for: TACGGTTGGCGAAGTCACATC; LANA Rev: CCTCGCAGCAGACTACACCTCCAC; ORF24 for: CGTGTTTTGTGGGTTCCAGC; ORF24 Rev: GGCGACGCTTTCAAGAATCC; K8.1 for: TCAGCCTTTTCAGGATCATATTCA; K8.1 Rev: CAGC AATAAACCCACAGCCC; vIRF-4 for: CCTGCCGGCAGCGATATCCCGCCT; vIRF-4 Rev: CAAATGC ATGGTACACCGAATACC; vIRF-1 for: CCGGACACGACAACTAAGAA; vIRF-1 Rev: GTCTCTGCG CCATTCAAAAC; IFN-α1 for: GGACCTTGATGCTCCTGGCACAAA; IFN-α1 Rev: TCTAGGAGGTC CTCATCCCAAGCA; IFN-β1 for: CAGTCCTGGAAGAAAAAC; IFN-β1 Rev: TCAGTTTCGGAGGT AACCTGT; GAPDH for: CCAGGTGGTCTCCTCTGACTTCTC; GAPDH Rev: ATACCAGGAAATGA GCTTGACA. The LANA primers were also used for qPCR of viral DNA.

Lentivirus production

For generation of lentivirus stocks, ~80%-confluent 293T cultures in 75-cm^2 flasks were transfected with 12 µg of lentiviral vector DNA, 9 µg of psPAX2 (Addgene 12260), and 3 µg of pMD2.G (Addgene 12259); the latter two packaging vectors were provided by Dr. Didier Trono. After application of DNA-PEI mixtures for >6 h, the medium was replaced, and incubation was continued for ~60 h. The virus-containing medium was harvested, virus pelleted by ultracentrifugation (25,000 rpm in an SW32Ti rotor for 2 h at 4°C), and virus pellets resuspended in 4 mL of DMEM containing 10% FBS before storage in aliquots at −80°C.

HHV-8 mutagenesis

Mutagenesis of the BAC16 bacmid genome of HHV-8 (22) was carried out using methods outlined previously (23), employing coinsertion of mutations and a kanamycin-resistance (Kan^r) cassette and subsequent removal of Kan^r sequences via intramolecular recombination. Both recombination steps were checked by PCR amplification of the appropriate genome locus, and intended genetic alterations were verified by sequencing. Wild-type-reverted (repaired) BAC16 genomes were generated similarly to provide controls in phenotypic analyses. Engineered viruses utilized in this study comprised those containing initiator-codon ATG-to-TTG (HHV-8.vIRF-4^X), those expressing STS_{214}AAA (HHV-8.vIRF-4.STS^X) and TWR_{233}AAA (HHV-8.vIRF-4.TWR^X) vIRF-4, repaired versions of the residue-substitution mutations (HHV-8.vIRF-4.STS^R and HHV-8.TWR^R), and viruses expressing Flag-tagged versions of vIRF-4, vIRF-4.STS^X, and vIRF-4.TWR^X. PCR primers contained the required mutations, sequences for amplification of the Kan^r cassette (from pEP-kanS; Addgene, 41017), and reiterated HHV-8 sequences (40 bp) for excision of Kan^r in the second recombination step. Fusion of 3xFlag-encoding sequences (GACTACAAGGACCACGACGGTGACTACAAGGA CCACGACATCGACTACAAGGACGACGA CGACAAGTGA) to the 3′-end of vIRF-4, vIRF-4.STS^X, and vIRF-4.TWR^X ORFs in BAC16 was undertaken by similar recombineering methods, employing overlapping PCR methods to generate the required PCR fragment for recombination with the respective BAC16 genomes. SpeI or HindIII restriction digestion and 0.8%-agarose gel electrophoresis (12V for ~20 h) were used to check the gross integrity of the recombinant genomes. Fugene 6 (Promega, E2691) was used to transfect the BAC16 genomes into iSLK cells, which were

selected in hygromycin (2.3 mM) for at least 2 weeks. The cultures were treated with doxycycline (1.9 nM) and sodium butyrate (1 mM) to induce lytic replication, and media were harvested after 5 days to provide virus stocks. These were titered, using GFP-positivity of the infected cells, to determine infectious doses and derive infection-normalized iSLK cultures for experimental use.

Immuno- and affinity-precipitations

Immuno- and affinity-precipitations of Flag, CBD, and S-tagged proteins from cell lysates of transfected cells (293T) or lentiviral vector-transduced cells (iSLK) were carried out using appropriate immuno- or affinity-beads (Flag: Sigma, M8823; CBD: New England Biolabs, S6651; S-protein: Novagen, 69704), according to the manufacturers' instructions. Cells were harvested ~48 h post-transfection; cultures used for ubiquitination studies were treated for 10 h with MG132 prior to harvest. Harvested cells were lysed in either regular lysis buffer [50 mM Tris-HCl (pH7.5), 150 mM NaCl, 5 mM EDTA, 0.2% NP40] containing a protease inhibitor cocktail (Sigma, P8340) or, for studies of ubiquitinated vIRF-4 and TRAF3, denaturing lysis buffer (Tris-buffered saline containing 1% SDS) for at least 30 minutes at 4°C, prior to micro-tip sonication (to disrupt nuclei/DNA) and extract clarification by centrifugation at 15,000 x g for 15 minutes at 4°C. SDS-denatured samples were boiled for 10 minutes and diluted 10-fold in TBS prior to clarification and use of supernatants for immuno- or affinity-precipitations. Incubations of lysates with immuno/affinity-beads were carried out overnight at 4°C, with gentle shaking. Bead-bound precipitates were washed several times in buffer [50 mM Tris-HCl (pH 7.5), 150 mM NaCl, 0.04% NP40]. Matrix-bound proteins were released into SDS-PAGE loading buffer by boiling at 95°C for 10 minutes before gel fractionation and immunoblotting.

Antibodies

Immunoblotting primary antibodies used in this study were as follows: USP7 (Invitrogen, MA5-31515); β-actin (Sigma, A5316); GAPDH (Invitrogen, TAB1001); LANA (Advanced Biotechnologies, 13–210-100); CBD (New England BioLabs, E8034S); Flag (Sigma, F1804); ubiquitin (Enzo Life Sciences, ADI-SPA-200-F); K48-polyubiquitin (Cell Signaling, 4289); HA (Sigma, H3663); TRAF3 (Cell Signaling Technology, 4729); p53 (Santa Cruz Biotechnology, sc-126); S-tag (Cell Signaling Technology, 12774); vIRF-1 rabbit polyclonal antiserum (provided by Dr. Gary Hayward); vIL-6 rabbit polyclonal antiserum (39). Secondary detection antibodies comprised HRP-conjugated anti-rabbit-IgG (Cell Signaling Technology, 7074) and anti-mouse IgG (Cell Signaling Technology, 7076).

Luciferase reporter experiments

For 293T cell-based reporter assays, cultures in 12-well plates were transfected (using PEI) with 65 ng ISRE-Luc reporter plasmid, 30 ng pRL-TK (Renilla luciferase normalization control), and 0.35 µg vIRF-4 or control expression vector, with or without cotransfected MAVS expression plasmid (0.35 µg). Cells were harvested 24 h post-transfection for luciferase assays. For reporter experiments in HHV-8$^+$ iSLK cells, transfections were effected using Lipofectamine 2000; after 6 h, the medium was replaced with DMEM containing doxycycline (1.9 nM) and sodium butyrate (1 mM) for lytic induction, and cells were harvested 24 h later for lysis and luciferase assays. Renilla (normalization control) and firefly luciferase activities were determined using commercial reagents (Promega, E2920) according to the manufacturer's instructions.

ACKNOWLEDGMENTS

We thank Drs. B. Stringer, T. Dawson, and D. Trono for provision of plasmids used in this study.

This work was supported by NIH grant R01AI140855 to J.N.

AUTHOR AFFILIATION

[1]Sidney Kimmel Comprehensive Cancer Center at Johns Hopkins, Department of Oncology, Johns Hopkins University School of Medicine, Baltimore, Maryland, USA

AUTHOR ORCIDs

John Nicholas http://orcid.org/0000-0002-4058-9652

FUNDING

Funder	Grant(s)	Author(s)
HHS | National Institutes of Health (NIH)	AI140855	John Nicholas

AUTHOR CONTRIBUTIONS

Zunlin Yang, Conceptualization, Data curation, Formal analysis, Investigation, Methodology, Project administration, Validation, Visualization, Writing – review and editing | John Nicholas, Conceptualization, Data curation, Funding acquisition, Methodology, Project administration, Resources, Supervision, Visualization, Writing – original draft, Writing – review and editing

ADDITIONAL FILES

The following material is available online.

Supplemental Material

Fig. S1 (JVI00255-24-s0001.tiff). Interferon-signaling regulation by vIRF-4 and USP7-binding variants.

Fig. S2 (JVI00255-24-s0002.tif). Effect of vIRF-4 ablation/depletion and vIRF-4-USP7 interaction on p53 expression.

REFERENCES

1. Cunningham C, Barnard S, Blackbourn DJ, Davison AJ. 2003. Transcription mapping of human herpesvirus 8 genes encoding viral interferon regulatory factors. J Gen Virol 84:1471–1483. https://doi.org/10.1099/vir.0.19015-0
2. Rivas C, Thlick AE, Parravicini C, Moore PS, Chang Y. 2001. Kaposi's sarcoma-associated herpesvirus LANA2 is a B-cell-specific latent viral protein that inhibits p53. J Virol 75:429–438. https://doi.org/10.1128/JVI.75.1.429-438.2001
3. Burýsek L, Pitha PM. 2001. Latently expressed human herpesvirus 8-encoded interferon regulatory factor 2 inhibits double-stranded RNA-activated protein kinase. J Virol 75:2345–2352. https://doi.org/10.1128/JVI.75.5.2345-2352.2001
4. Dittmer DP. 2003. Transcription profile of Kaposi's sarcoma-associated herpesvirus in primary Kaposi's sarcoma lesions as determined by real-time PCR arrays. Cancer Res 63:2010–2015.
5. Baresova P, Pitha PM, Lubyova B. 2013. Distinct roles of Kaposi's sarcoma-associated herpesvirus-encoded viral interferon regulatory factors in inflammatory response and cancer. J Virol 87:9398–9410. https://doi.org/10.1128/JVI.03315-12
6. Koch S, Schulz TF. 2017. Rhadinoviral interferon regulatory factor homologues. Biol Chem 398:857–870. https://doi.org/10.1515/hsz-2017-0111
7. Hwang SW, Kim D, Jung JU, Lee HR. 2017. KSHV-encoded viral interferon regulatory factor 4 (vIRF4) interacts with IRF7 and inhibits interferon alpha production. Biochem Biophys Res Commun 486:700–705. https://doi.org/10.1016/j.bbrc.2017.03.101
8. Ma Z, Jacobs SR, West JA, Stopford C, Zhang Z, Davis Z, Barber GN, Glaunsinger BA, Dittmer DP, Damania B. 2015. Modulation of the cGAS-STING DNA sensing pathway by gammaherpesviruses. Proc Natl Acad Sci U S A 112:E4306–E4315. https://doi.org/10.1073/pnas.1503831112
9. Robinson BA, O'Connor MA, Li H, Engelmann F, Poland B, Grant R, DeFilippis V, Estep RD, Axthelm MK, Messaoudi I, Wong SW. 2012. Viral interferon regulatory factors are critical for delay of the host immune response against rhesus macaque rhadinovirus infection. J Virol 86:2769–2779. https://doi.org/10.1128/JVI.05657-11
10. Heinzelmann K, Scholz BA, Nowak A, Fossum E, Kremmer E, Haas J, Frank R, Kempkes B. 2010. Kaposi's sarcoma-associated herpesvirus viral interferon regulatory factor 4 (vIRF4/K10) is a novel interaction partner of CSL/CBF1, the major downstream effector of Notch signaling. J Virol 84:12255–12264. https://doi.org/10.1128/JVI.01484-10
11. Lee HR, Mitra J, Lee S, Gao SJ, Oh TK, Kim MH, Ha T, Jung JU. 2016. Kaposi's sarcoma-associated herpesvirus viral interferon regulatory factor 4 (vIRF4) perturbs the G1-S cell cycle progression via deregulation of the cyclin D1 gene. J Virol 90:1139–1143. https://doi.org/10.1128/JVI.01897-15
12. Xi X, Persson LM, O'Brien MW, Mohr I, Wilson AC. 2012. Cooperation between viral interferon regulatory factor 4 and RTA to activate a subset of Kaposi's sarcoma-associated herpesvirus lytic promoters. J Virol 86:1021–1033. https://doi.org/10.1128/JVI.00694-11
13. Chavoshi S, Egorova O, Lacdao IK, Farhadi S, Sheng Y, Saridakis V. 2016. Identification of Kaposi sarcoma herpesvirus (KSHV) vIRF1 protein as a novel interaction partner of human deubiquitinase USP7. J Biol Chem 291:6281–6291. https://doi.org/10.1074/jbc.M115.710632
14. Xiang Q, Ju H, Li Q, Mei SC, Chen D, Choi YB, Nicholas J. 2018. Human herpesvirus 8 interferon regulatory factors 1 and 3 mediate replication and latency activities via interactions with USP7 deubiquitinase. J Virol 92:e02003-17. https://doi.org/10.1128/JVI.02003-17
15. Xiang Q, Ju H, Nicholas J. 2020. USP7-dependent regulation of TRAF activation and signaling by a viral interferon regulatory factor homologue. J Virol 94:e01553-19. https://doi.org/10.1128/JVI.01553-19

16. Lee HR, Choi WC, Lee S, Hwang J, Hwang E, Guchhait K, Haas J, Toth Z, Jeon YH, Oh TK, Kim MH, Jung JU. 2011. Bilateral inhibition of HAUSP deubiquitinase by a viral interferon regulatory factor protein. Nat Struct Mol Biol 18:1336–1344. https://doi.org/10.1038/nsmb.2142
17. Tavana O, Gu W. 2017. Modulation of the p53/MDM2 interplay by HAUSP inhibitors. J Mol Cell Biol 9:45–52. https://doi.org/10.1093/jmcb/mjw049
18. Aloni-Grinstein R, Charni-Natan M, Solomon H, Rotter V. 2018. p53 and the viral connection: back into the future ‡ Cancers (Basel) 10:53. https://doi.org/10.3390/cancers10060178
19. Sato Y, Tsurumi T. 2013. Genome guardian p53 and viral infections. Rev Med Virol 23:213–220. https://doi.org/10.1002/rmv.1738
20. Lazo PA, Santos CR. 2011. Interference with p53 functions in human viral infections, a target for novel antiviral strategies? Rev Med Virol 21:285–300. https://doi.org/10.1002/rmv.696
21. Koch S, Damas M, Freise A, Hage E, Dhingra A, Rückert J, Gallo A, Kremmer E, Tegge W, Brönstrup M, Brune W, Schulz TF. 2019. Kaposi's sarcoma-associated herpesvirus vIRF2 protein utilizes an IFN-dependent pathway to regulate viral early gene expression. PLoS Pathog 15:e1007743. https://doi.org/10.1371/journal.ppat.1007743
22. Brulois KF, Chang H, Lee AS-Y, Ensser A, Wong L-Y, Toth Z, Lee SH, Lee H-R, Myoung J, Ganem D, Oh T-K, Kim JF, Gao S-J, Jung JU. 2012. Construction and manipulation of a new Kaposi's sarcoma-associated herpesvirus bacterial artificial chromosome clone. J Virol 86:9708–9720. https://doi.org/10.1128/JVI.01019-12
23. Tischer BK, Smith GA, Osterrieder N. 2010. En passant mutagenesis: a two step markerless red recombination system. Methods Mol Biol 634:421–430. https://doi.org/10.1007/978-1-60761-652-8_30
24. Myoung J, Ganem D. 2011. Generation of a doxycycline-inducible KSHV producer cell line of endothelial origin: maintenance of tight latency with efficient reactivation upon induction. J Virol Methods 174:12–21. https://doi.org/10.1016/j.jviromet.2011.03.012
25. Kwon YT, Ciechanover A. 2017. The ubiquitin code in the ubiquitin-proteasome system and autophagy. Trends Biochem Sci 42:873–886. https://doi.org/10.1016/j.tibs.2017.09.002
26. Yau R, Rape M. 2016. The increasing complexity of the ubiquitin code. Nat Cell Biol 18:579–586. https://doi.org/10.1038/ncb3358
27. Lee HR, Toth Z, Shin YC, Lee JS, Chang H, Gu W, Oh TK, Kim MH, Jung JU. 2009. Kaposi's sarcoma-associated herpesvirus viral interferon regulatory factor 4 targets MDM2 to deregulate the p53 tumor suppressor pathway. J Virol 83:6739–6747. https://doi.org/10.1128/JVI.02353-08
28. Chen J, Ueda K, Sakakibara S, Okuno T, Yamanishi K. 2000. Transcriptional regulation of the Kaposi's sarcoma-associated herpesvirus viral interferon regulatory factor gene. J Virol 74:8623–8634. https://doi.org/10.1128/jvi.74.18.8623-8634.2000
29. Bu W, Palmeri D, Krishnan R, Marin R, Aris VM, Soteropoulos P, Lukac DM. 2008. Identification of direct transcriptional targets of the Kaposi's sarcoma-associated herpesvirus Rta lytic switch protein by conditional nuclear localization. J Virol 82:10709–10723. https://doi.org/10.1128/JVI.01012-08
30. Lin M, Ji X, Lv Y, Cui D, Xie J. 2023. The roles of TRAF3 in immune responses. Dis Markers 2023:7787803. https://doi.org/10.1155/2023/7787803
31. Kumar A, Salemi M, Bhullar R, Guevara-Plunkett S, Lyu Y, Wang KH, Izumiya C, Campbell M, Nakajima KI, Izumiya Y. 2021. Proximity biotin labeling reveals Kaposi's sarcoma-associated Herpesvirus interferon regulatory factor networks. J Virol 95:e02049-20. https://doi.org/10.1128/JVI.02049-20
32. Nakamura H, Lu M, Gwack Y, Souvlis J, Zeichner SL, Jung JU. 2003. Global changes in Kaposi's sarcoma-associated virus gene expression patterns following expression of a tetracycline-inducible Rta transactivator. J Virol 77:4205–4220. https://doi.org/10.1128/jvi.77.7.4205-4220.2003
33. Yang Z, Xiang Q, Nicholas J. 2023. Direct and biologically significant interactions of human herpesvirus 8 interferon regulatory factor 1 with STAT3 and Janus kinase TYK2. PLoS Pathog 19:e1011806. https://doi.org/10.1371/journal.ppat.1011806
34. Choi YB, Choi Y, Harhaj EW. 2018. Peroxisomes support human herpesvirus 8 latency by stabilizing the viral oncogenic protein vFLIP via the MAVS-TRAF complex. PLoS Pathog 14:e1007058. https://doi.org/10.1371/journal.ppat.1007058
35. Ishikawa H, Barber GN. 2008. STING is an endoplasmic reticulum adaptor that facilitates innate immune signalling. Nature 455:674–678. https://doi.org/10.1038/nature07317
36. Chen D, Nicholas J. 2015. Promotion of endoplasmic reticulum-associated degradation of procathepsin D by human herpesvirus 8-encoded viral interleukin-6. J Virol 89:7979–7990. https://doi.org/10.1128/JVI.00375-15
37. Lim KL, Chew KCM, Tan JMM, Wang C, Chung KKK, Zhang Y, Tanaka Y, Smith W, Engelender S, Ross CA, Dawson VL, Dawson TM. 2005. Parkin mediates nonclassical, proteasomal-independent ubiquitination of synphilin-1: implications for Lewy body formation. J Neurosci 25:2002–2009. https://doi.org/10.1523/JNEUROSCI.4474-04.2005
38. Chen D, Sandford G, Nicholas J. 2009. Intracellular signaling mechanisms and activities of human herpesvirus 8 interleukin-6. J Virol 83:722–733. https://doi.org/10.1128/JVI.01517-08
39. Wan X, Wang H, Nicholas J. 1999. Human herpesvirus 8 interleukin-6 (vIL-6) signals through gp130 but has structural and receptor-binding properties distinct from those of human IL-6. J Virol 73:8268–8278. https://doi.org/10.1128/JVI.73.10.8268-8278.1999